

Synchronization of rescaled adaptive coupling and its application to shock capturing

G. W. Wei

*Department of Computational Science, National University of Singapore
Singapore 117543, R. Singapore
(February 8, 2008)*

This Letter proposes a rescaled adaptive coupling scheme for the synchronization of spatially extended systems. Coupling and synchronization are analyzed from the point view of image filter construction. A length rescaling technique is introduced based on dimensional argument of control process. Control sensors are adaptively selected according to local information. The coupling strength on each sensor is automatically adjusted according to the magnitude of local oscillations. We demonstrate that the present scheme can efficiently suppress and control spatiotemporal oscillations and thus, provide a powerful approach for shock capturing. Both the Navier-Stokes equation describing shear layer flows around a jet and Burgers' equation are solved to illustrate the idea.

PACS numbers: 05.45.+b, 02.70.-c, 47.40.Nm

Synchronization phenomenon is of fundamental importance in telecommunication [1], electronic circuits [2], nonlinear optics [3], and chemical and biological systems [4]. The phenomenon has been studied extensively both by numerical and experimental means. It is believed that an in-depth study and understanding of synchronization will greatly benefit the advancement of science and technology. Different types of synchronization, such as identical [5,1], generalized [6], lag and phase synchronization [7], were proposed. Recently, synchronization and control of spatially extended systems have received great attention [8,9]. For a given system, the degree and rate of synchronization depends vitally on the coupling scheme used. A variety of coupling schemes, such as unidirectional coupling, receptor-product coupling, weak coupling, strong coupling, global coupling, and local coupling, have been studied. However, adaptively coupled schemes and their effect on the rate and degree of synchronization have not been addressed yet. Moreover, very little is reported on synchronization with respect to the understanding of nonlinear hyperbolic conservation laws, shock capturing and, in general, computational methodology. The latter has had tremendous impact to a variety of disciplines in science and engineering. In fact, much of the present understanding on synchronization was achieved with the aid of numerical computations.

The main purpose of this Letter is to introduce rescaled adaptively coupled synchronization schemes and to use them for shock capturing. A local gradient based coupling scheme is introduced for continuous systems. Nondecreasing functions and non-increasing functions are designed for oscillation reduction and image edge preservation, respectively. We demonstrate that appropriate coupling of two identical dynamical systems can result in a surprisingly novel and efficient scheme for shock capturing. The validity and efficiency of this scheme is tested by using an inviscid Burgers' equation and the Navier-Stokes equation for incompressible flows.

For simplicity, we consider an identical synchronization, where two coupled systems are exactly of the same type and can be given by a partial differential equation of the form

$$u_t = F(u, u_x, u_{xx}, \dots) + c(u, w), \quad (1)$$

where $c(u, w)$ is a dissipative coupling term, which is proportional to the difference between the states of two systems, $(u - w)$. Based on an experimental consideration, Junge and Partitz [9] proposed a sensor coupling scheme, which utilizes the difference between two spatially averaged local signals $(\bar{u} - \bar{w})$. Here, $\bar{w}(x, t) = \frac{1}{l} \int_{x-l/2}^{x+l/2} w(y, t) dy$ is the local average of w over a length l at the position of a sensor. It is noted that a dimensional scaling effect has to be accounted when the solution of a partial differential equation is related to an experimental measurement. In fact, in control experiments, two coupled systems might have very different spatial extensions (the control part is usually much smaller in size, e.g., a human brain vs human body). Mathematically, the dimensionless partial differential equation usually has one or more parameters which contain the length scale. We argue that, when two dynamical systems characterized by different values of a parameter are coupled together, one of the two dynamical systems should be appropriately rescaled. Therefore, we propose a rescaled coupling scheme

$$c(u, w) \propto (u - \bar{w}), \quad (2)$$

where \bar{w} is a local average of w . It is important to understand that the coupling between two systems given by Eq. (2) is generally designed as a dissipative coupling. However, an interesting observation can be made at the limit of complete identical synchronization (i.e. the strong convergence of the two systems $\|u(t) - w(t)\| \rightarrow 0$ for $t \rightarrow \infty$). From the point of view of image processing, the local average \bar{w} is equivalent to the treatment of w by a low-pass filter. Moreover, at the limit of complete identical synchronization, $(u - \bar{w})$ is equivalent to the treatment of u by a high-pass

filter [10]. There is a similar effect on the second system under the same condition. As such, the rescaled sensor coupling expression given by Eq. (2) can be used for image processing, pattern recognition and shock capturing. In these applications, spatially selected treatment is of practical importance. To achieve spatial selectivity, we introduce following rescaled and adaptively distributed local sensors

$$c(u, w) \propto \varepsilon(|u_x|)(u - \bar{w}), \quad (3)$$

where the coupling strength ε is a function of the gradient measurement $|u_x|$. For the purpose of edge-detected pattern recognition, we choose $\varepsilon(|u_x|)$ as a non-increasing function, e.g.

$$\varepsilon(|u_x|) = \epsilon \exp\left[-\frac{|u_x|^2}{2\sigma^2}\right], \quad (4)$$

where ϵ and σ are constants. For the purpose of noise reduction and oscillation suppression, we choose $\varepsilon(|u_x|)$ as a nondecreasing function, e.g.

$$\varepsilon(|u_x|) = \epsilon |u_x|^{\frac{1}{4}}, \quad (5)$$

where ϵ is a constant. Obviously many other nondecreasing functions can also be used. In the rest of the Letter we restrict ourselves to the application of the present synchronization scheme to shock capturing.

The solution of the inviscid Burgers' equation and the incompressible Navier-Stokes equations for very high Reynolds numbers is often difficult to attain due to the possible existence of shock front. Shock wave is a common phenomenon in nature, such as in aerodynamics and hydrodynamics, and is usually described by hyperbolic conservation laws and by inviscid hydrodynamic equations. The construction of numerical schemes that are capable of efficient shock capturing is a challenging task.

To illustrate our synchronization approach for oscillation reduction, we first consider Burgers' model of turbulence

$$u_t + uu_x = \frac{1}{\text{Re}} u_{xx}, \quad (6)$$

where $u(x, t)$ is the dependent variable resembling the flow velocity and Re is the Reynolds number characterizing the size of the viscosity. Burgers' equation is an important model for the understanding of physical flows. The competition between the nonlinear advection and the viscous diffusion is controlled by the value of Re in Burgers' equation, and thus determines the behavior of the solution. We consider Eq. (6) using the following initial and boundary conditions

$$u(x, 0) = \sin(\pi x), \quad u(0, t) = u(1, t) = 0. \quad (7)$$

The forth order Runge-Kutta scheme is used for the temporal discretization with a time increment $\Delta t = 0.002$. A discrete singular convolution (DSC) algorithm [11,12] is utilized for spatial discretization with a total of 101 grid points in the computational domain. The use of DSC algorithm for solving differential equations has been extensively tested and further validation is given in TABLE I.

Solving Burgers' equation at a high Reynolds number is a challenging task. At a Reynolds number of 10^3 , the numerical solution quickly develops into a sharp shock front near $x = 1$. Severe oscillations occur near the shock front as shown in FIG. 1a. It should be pointed out that, almost all high order numerical schemes exhibit similar oscillations. To eliminate oscillations, we employ the rescaled adaptive coupling, Eq.(5), in solving Burgers' equation (6). Here \bar{w} is computed by a local three-term average. Two systems, which are characterized by two Reynolds numbers ($\text{Re}_1 = 1000$ and $\text{Re}_2 = 100$), are coupled with a coupling constant of $\epsilon = -80$. It can be seen from FIG. 1b that all spurious oscillations could be eliminated. However, the synchronized solution is neither the true solution of $\text{Re} = 100$ nor that of $\text{Re} = 1000$. Hence, it is desirable to have an oscillation-free solution at a given high Reynolds number. To this end, we design an *autosynchronization* approach by choosing two exactly identical systems, i.e., setting $\text{Re}_1 = \text{Re}_2 = \infty$. As two exactly identical systems are still coupled, oscillations are suppressed to a certain degree, depending on the coupling constant. For a relatively small coupling constant of $\epsilon = -40$, the solution is oscillatory at early times and become essentially non-oscillatory at a later time (see FIG. 1c). By increasing the coupling constant to $\epsilon = -90$, we have successfully eliminated all spurious oscillations as shown in FIG. 1d.

To validate the present approach further, we consider the two dimensional Navier-Stokes equation

$$\mathbf{U}_t + \mathbf{U} \cdot \nabla \mathbf{U} = -\nabla p + \frac{1}{\text{Re}} \nabla^2 \mathbf{U} + \varepsilon(|\nabla \mathbf{U}|)(\mathbf{U} - \bar{\mathbf{W}}) \quad (8)$$

with the incompressible condition, $\nabla \cdot \mathbf{U} = 0$. Here $\mathbf{U} = (u, v)^T$ is the velocity vector, \mathbf{W} is the velocity vector of the second system, p is the pressure, Reynolds number of $\text{Re} = \infty$ defines the Euler equation. The domain of interest is

a square $[0, 2\pi] \times [0, 2\pi]$ with periodic boundary conditions. Depending on the initial values, this system can be very challenging to solve. For smooth initial values, the solution scheme and the validity of the DSC algorithm were tested in Ref. [12]. With appropriate initial values, the Euler equation ($\text{Re} = \infty$) can be used to describe the flow field of vertically perturbed horizontal shear layers around a jet.

We now test our synchronization approach for the Euler equation with sharply varying initial values. This example is chosen to illustrate the ability of the present approach for providing very fine resolution even on a relatively coarse grid. The initial values are that of a jet in a doubly periodic geometry

$$\begin{aligned} u(x, y, 0) &= \begin{cases} \tanh\left(\frac{2y-\pi}{2\rho}\right), & \text{if } y \leq \pi \\ \tanh\left(\frac{3\pi-2y}{2\rho}\right), & \text{if } y > \pi \end{cases} \\ v(x, y, 0) &= \delta \sin(x), \end{aligned} \tag{9}$$

where $\delta = 0.05$ is used for the convenience of comparison with the previous study [13,14]. This initial value describes the flow field consisting of horizontal shear layers of finite thickness, perturbed by a small amplitude vertical velocity, making up the boundaries of the jet. However, this problem is not analytically solvable. Pioneering work was done by Bell et al [13] in this field, in which they utilized a second-order Godunov scheme in association with a projection approach for divergence-free velocity field with a general boundary condition. A state of the art high-order essentially non-oscillatory (ENO) scheme was constructed by E and Shu [14] to resolve the fine vorticity structure of the double shear layers with periodic boundary conditions.

We consider the parameter $\rho = \pi/15$, a case studied by Bell et al [13] using a projection method with three sets of grids (128^2 , 256^2 and 512^2). E and Shu [14] computed this case by using both spectral collocation code with 512^2 points and their high order ENO scheme with 64^2 and 128^2 points. The spectral collocation code produced an oscillatory solution at $t = 10$ (see FIG. 1 of Ref. [14]), while the high order ENO scheme produced a defect at $t = 6$ as the channels connecting the vorticity centers are slightly distorted (see FIG. 2 of Ref. [14]). In the present simulation, we choose a 64^2 grid for the computational domain with a time increment of 0.002. The synchronization prescription given in Eq. (5) is used with a coupling constant of $\epsilon = -80$. The results at different times ($t=4,6,8$, and 10) are plotted in FIG 2. It is seen that our solution is smooth (some non-smooth features in the contour plot are attributed to the coarse grid employed in the study) and stable for this case. In particular, no distortion is found in vorticity contours at $t=6$. For early times, present results compare extremely well with those of the spectral collocation code computed with 512^2 points. There are no spurious numerical oscillations during the entire process.

In conclusion, we propose the approach of synchronization as a robust, reliable and practical algorithm for shock wave computations. A length rescaling technique is introduced based on the dimensional argument of control process. To achieve computational efficiency and reliability, coupling sensors in spatially extended systems are adaptively selected according to local information. The coupling strength at each sensor is adaptively varied according to the magnitude of the local gradient of the system. The resulting coupled systems are analyzed from point of view of image filters. The proposed algorithm is validated by using Burgers' equation and the incompressible Navier-Stokes equation. A high accuracy discrete singular convolution algorithm [11,12] is utilized for the numerical simulation.

For Burgers' equation, we have tested the computational accuracy and reliability at a moderately high Reynolds number. At high Reynolds numbers, Burgers' equation is difficult to solve. We first test the synchronization approach in two systems for different Reynolds numbers. One of the two systems develops spurious oscillations which could be eliminated by coupling to a low Reynolds number system. The oscillations are completely suppressed at synchronization. To make the algorithm practical for shock capturing at any given Reynolds number, we couple two truly identical systems (i.e., the same dynamical system, the same parameters). It was found that the oscillations could be completely eliminated above a suitable minimum coupling strength.

To further validate the present synchronization approach for shock capturing in practical large scale computations, we consider the simulation of doubly periodic shear layer flows. For this purpose, the Navier-Stokes equation with appropriate initial and boundary conditions is employed. Numerical simulation of this system is an acid test for ordinary methods, including spectral methods. Our synchronization scheme performs extremely well. With a relatively small grid mesh, the present results are better than those of a state of the art shock capturing scheme, the high order essentially non-oscillatory (ENO) scheme [14], obtained over a much larger grid mesh. This indicates that the proposed approach has a great potential for being used as an efficient and reliable algorithm for the practical simulation of fluid flows and computational physics in general. Progress has been made on the application of the present synchronization approach to image processing.

This work was supported in part by the National University of Singapore.

- [1] L. Kocarev and U. Parlitz, Phys. Rev. Lett. **74**, 5028 (1995).
- [2] V. S. Anischenko, T. E. Vadivasova, D. E. Postnov, and M. A. Safonova, Int. J. Bifurcation Chaos Appl. Sci. Eng. **2**, 633 (1992); J. F. Heagy, T. L. Carroll, and L. M. Pecora, Phys. Rev. A **50**, 1874 (1994).
- [3] L. Fabiny, P. Colet, and R. Roy, Phys. Rev. A **47**, 4287 (1993); R. Roy and K. S. Thornburg, Jr., Phys. Rev. Lett. **72**, 2009 (1994).
- [4] I. Schreiber and M. Marek, Physica (Amsterdam) **5D**, 258 (1982); S. K. Han, C. Kurrer, and Y. Kuramoto, Phys. Rev. Lett. **75**, 3190 (1995).
- [5] H. Fujisaka and T. Yamada, Prog. Theor. Phys. **69**, 32 (1983).
- [6] N. Rulkov, M. Sushchik, L. Tsimering, and H. Abarbanel, Phys. Rev. E **51**, 980 (1995); L. Kocarev and U. Parlitz, Phys. Rev. Lett. **76**, 1816 (1996).
- [7] M. G. Rosenblum, A. Pikovsky, and J. Kurths, Phys. Rev. Lett. **76**, 1816 (1996); U. Parlitz, L. Junge, W. Lauterborn, and L. Kocarev, Phys. Rev. E **54**, 2115 (1996).
- [8] J. H. Xiao, G. Hu, J. Z. Yang, and J. H. Gao, Phys. Rev. Lett. **81**, 5552 (1998); S. Boccaletti, J. Bragard, F. T. Arecchi, and H. Mancini, Phys. Rev. Lett. **83**, 536 (1999); B. Blasius, A. Huppert, and L. Stone, Nature **399**, 354 (1999).
- [9] L. Junge and U. Parlitz, Phys. Rev. E **61**, 3736 (2000).
- [10] R. G. Ganzalez and R. E. Woods, *Digital Image Processing*, p196, (Addison-Wesley Company, Inc. New York, 1993).
- [11] G. W. Wei, J. Chem. Phys. **110**, 8930 (1999); G. W. Wei, Physica D **137**, 247 (2000); G. W. Wei, J. Phys. B **33**, 343 (2000).
- [12] G. W. Wei, J. Phys. A, **33**, 4935 (2000); G. W. Wei, Computer Meth. Appl. Mech. Engng. in press.
- [13] J. B. Bell, P. Cilella and H. M. Glaz, J. Comput. Phys. **85**, 257 (1989).
- [14] W. E and C.-W. Shu, J. Comput. Phys., **110**, 39 (1994).

TABLE I. L_1 and L_∞ errors of the DSC solutions for Burgers' equation

t	0.4	1.2	2.0	3.0	10	20	40
L_1	2.1(-4)	4.2(-5)	9.4(-7)	3.8(-8)	1.5(-11)	3.2(-12)	4.1(-13)
L_∞	2.8(-3)	6.8(-4)	1.2(-5)	4.0(-7)	4.0(-11)	5.3(-12)	6.4(-13)

Figure Captions

FIG. 1. Synchronization profiles of Burgers' equation at $t=0.2$ (i), 0.4 (ii), 0.6 (iii), 1.2 (iv) and 2.0 (v). (a) $\epsilon = 0$, solid line: $Re_1=1000$, dots: $Re_2=100$; (b) $\epsilon = -80$, solid line: $Re_1=1000$, dots: $Re_2=100$; (c) $\epsilon = -40$, $Re_1=Re_2=\infty$; (d) $\epsilon = -90$, $Re_1=Re_2=\infty$.

FIG. 2. The vorticity contours of the synchronization solution of the 2D Euler equation with 64^2 points. Up left: $t = 4$; up right: $t = 6$; low left: $t = 8$; low right: $t = 10$.

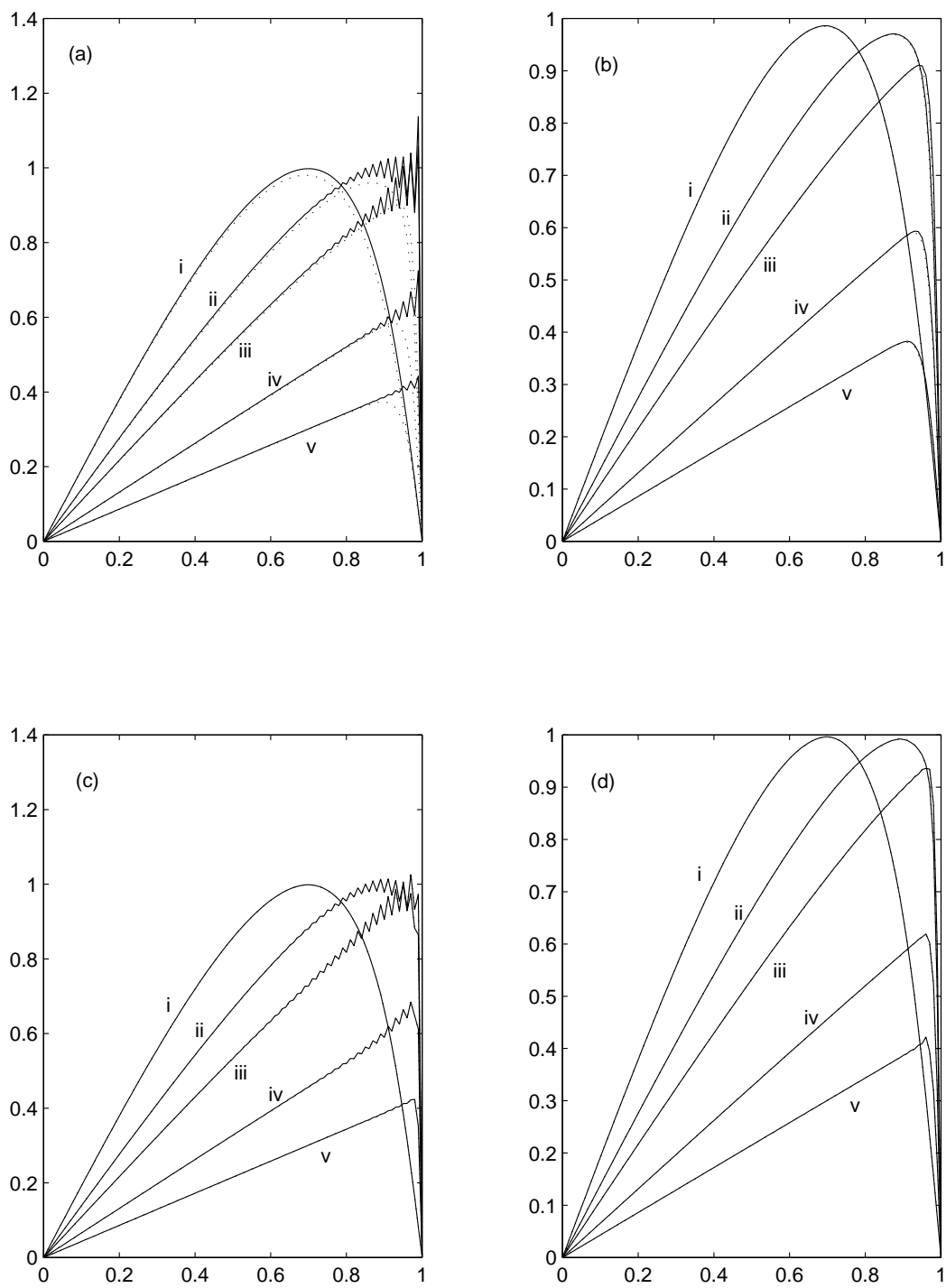


FIG. 1

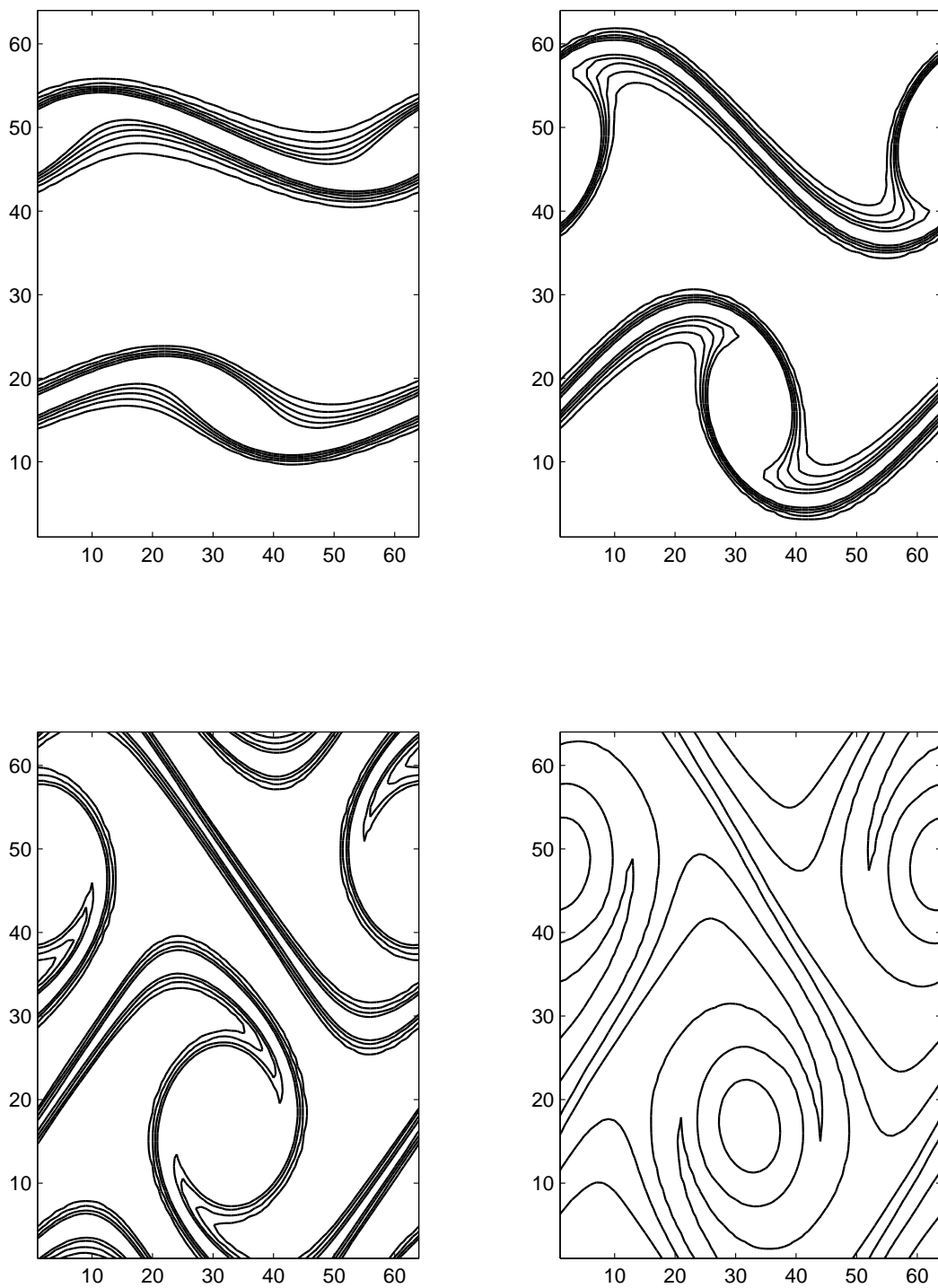


FIG. 2